

Optimal Viewpoint Finding for 3D Visualization of Spatio-temporal Vehicle Trajectories on Caution Crossroads Detected from Vehicle Recorder Big Data

Masahiko Itoh*, Daisaku Yokoyama[†], Masashi Toyoda[†], and Masaru Kitsuregawa[‡]

*The University of Tokyo, National Institute of Information and Communications Technology, Email: imash@tkl.iis.u-tokyo.ac.jp

[†]The University of Tokyo, Email: {yokoyama,toyoda}@tkl.iis.u-tokyo.ac.jp

[‡]National Institute of Informatics, The University of Tokyo, Email: kitsure@tkl.iis.u-tokyo.ac.jp

Abstract—Traffic accidents are still troubling our society. The number of drive recorders sold has increased, and therefore we can collect large-scale vehicle recorder data to be used to support traffic safety. We have developed a system for detecting potentially risky crossroads on the basis of vehicle recorder data, road shapes, and weather information. Visualization combining space and time in a single display called a “space time cube (STC)” helps us to understand and analyze spatio-temporal mobility data on caution crossroads. The STC enables us to simultaneously explore not only shapes and positions of vehicle trajectories but also their temporal distributions. However, it is difficult for users to manually find good viewpoints for understanding such characteristics of trajectories. In this paper, we propose an optimal viewpoint selection method for visualizing spatio-temporal characteristics of vehicle trajectories on a large set of crossroads using an STC. Major contributions of this paper are as follows: (1) We provide an algorithm based on viewpoint entropy weighted by angles of trajectories with a horizontal line as a measure of a viewpoint quality on a projected 2D image. (2) We demonstrate our solution can be adapted to crossroads with different trajectory shapes. We also extend the proposed method to find an optimal viewpoint for multiple crossroads. (3) We verify the proposed method through users’ evaluations. (4) We construct an over-viewing catalog of potentially risky crossroads detected from real vehicle recorder big data to discuss and analyze them with stakeholders.

I. INTRODUCTION

A total of 499, 201 traffic accidents occurred in Japan according to recent transportation statistics in 2016¹. Traffic accidents are still troubling our society. Precise traffic safety support for drivers and pedestrians based on data such as driving data is required to further reduce the number of accidents.

The number of drive recorders sold domestically has increased about three times compared to three years ago, and has reached 790, 000 to date in Japan². This makes it possible for us to collect large-scale vehicle recorder data that can be used for traffic safety support. If we collect many

drivers’ records over a long time, the data will allow us to explore caution spots for driving on the basis of spatio-temporal driving data.

Visualization helps us to understand and analyze such spatio-temporal mobility data. Much research has been conducted on spatio-temporal analysis and visualization of mobility data [1], [2], [3], [4], [5], [6], [7], [8]. Some systems add a third axis to represent time. Visualization combining space and time in a single display was originally proposed by Hägerstrand [9], and is sometimes called a “space time cube (STC)”. In an STC, movements with latitude, longitude, and time become trajectories in a 3D space.

Amini et al. provided an experimental comparison of 2D and 3D visualizations of movement data to reveal advantages and disadvantages of 2D and 3D visualizations [10]. From a comparison with 2D visualization using a time slider, they found that an STC has an advantage of exploring temporal information. However, the users spent much time rotating the camera view in the STC. The STC requires more panning and rotating compared to the 2D. Camera angle reorganization is crucial for the STC to get good viewpoints for understanding targets.

Some research has been conducted on viewpoint selection for general 3D meshes and volume rendering [11], [12], [13]. Lee et al. and Tao et al. have studied viewpoint selection for flow visualization [14], [15]. Although their studies focused on streamline selection and viewpoint selection to identify salient flow regions, our study focused on viewpoint selection to understand both the shape of streamline on a map and the streamline distribution on a time axis.

We have developed systems for exploring caution spots from vehicle recorder big data [16]. We also have developed a method for detecting crossroads with potential risks on the basis of vehicle recorder data, road shapes, and weather information. After ranking potentially risky crossroads, we analyzed the detected crossroads with stakeholders in detail from the following aspects:

- What kind of road structures are detected as caution crossroads?
- What kind of caution operations occurred on the detected crossroads?

¹Cabinet Office, Government of Japan: http://www8.cao.go.jp/koutu/taisaku/h29kou_haku/index_zenbun_pdf.html#h28 (in Japanese)

²GfK: <http://www.gfk.com/jp/insights/press-release/1717drivingrecorder/> (in Japanese)

- What kind of trajectories did the caution operations occur on?
- At what time of the day did they occur?

For these purposes, visualization of both spatial structure and temporal distribution of vehicle trajectories is required. We therefore adapt space time cube visualization to our system. However, it is difficult for users to manually find good viewpoints that well display both spatial and temporal characteristics of vehicle trajectories for observing them on a map. This is especially difficult when there are a lot of crossroads. We need a method for automatically selecting optimal viewpoints in STC.

Our major contributions are as follows:

- We propose a novel method for automatically selecting optimal viewpoints for visualizing spatio-temporal characteristics of trajectories on a crossroad using an STC. For this purpose, we provide an algorithm based on viewpoint entropy weighted by angles with a horizontal line as a measure of a viewpoint quality of rendered trajectories on a projected image. As far as we know, there has been no research on viewpoint selection for visualizations of trajectories using an STC.
- We demonstrate our solution can be adapted to crossroads with different trajectory shapes. We also show the proposed method can be extended to find an optimal viewpoint for multiple crossroads to compare them from the same angle.
- We verify the presented method through users' evaluations. For this purpose, we manually rank the viewpoints through Scheffe's paired comparison, and measure Spearman's rank correlation coefficient between rankings defined by the proposed method and by users.
- We construct an overviewing catalog of caution crossroads detected from real vehicle recorder big data to discuss and analyze them with stakeholders of the data for evaluating the usability of the method.

In what follows, we give an outline of related work in Section II. We next introduce our approach for viewpoint selection based on the viewpoint entropy in Section III. Section IV provides users' evaluation results. We present case studies adapting the proposed method to detect caution crossroads from actual vehicle recorder big data in Section V. We conclude the paper in Section VI with a summary.

II. RELATED WORK

Much research has been conducted on visualization of mobility data collected by tracking technologies such as GPS using 2D visualization space [1], [2], [3], [4] and 3D visualization space [5], [7], [8]. Andrienko et al. extracted and characterized important places from mobility data such as GPS tracks of cars and flight trajectories and visualized them in 2D/3D spatio-temporal space [4], [5], [6]. However, most of them focused on analyzing traffic jams or movement

patterns. SAFETY MAP³ independently plots locations in which traffic accidents occurred and drivers suddenly braked. G Map⁴ plots points in which rapid acceleration occurred. However, they did not provide a function for exploring spatio-temporal characteristics of dangerous places. For this purpose, a space time cube visualization approach is required. Moreover, they did not provide a function for overviewing a lot of dangerous places to compare them in detail.

A number of approaches have been developed for overviewing a lot of 3D scenes, such as a catalog page for visualization results [17], [18], [19], [20], [21]. Worldlets [17] captures a 3D representation of a virtual environment landmark into a 3D thumbnail. It can provide catalogs for landmarks in the virtual environment. WorldBottle [18] made it possible to embed other spaces inside and render them on their surface, so that users can simultaneously compare multiple information spaces. Itoh et al. proposed a spreadsheet-based visualization framework for end-users to generate and modify multiple 3D visualizations [19]. They can provide multiple visualizations at the same time, but still have difficulty in finding good viewpoints for avoiding occlusions. It is difficult for users to find a good viewpoint for a 3D visualization, especially in multiple visualizations.

Many interactive techniques have been developed to deal with the occlusion reduction problem using different approaches [22]. Elmqvist et al. presented five design patterns for occlusion management based on a classification of existing interaction techniques such as multiple viewports, virtual X-ray, tour planners, volumetric probes, and projection distorters. Our purpose is not simply occlusion reduction, but to find a good viewpoint to understand spatio-temporal characteristics of the target spaces without deforming the targets and spaces. For this purpose, an approach for tour planners or viewpoint selection is required.

Research has been carried out on viewpoint selection for general 3D meshes and volume rendering [11], [23], [12], [13]. One solution for viewpoint selection for 3D meshes is the viewpoint entropy formulated by Vázquez et al. to evaluate the balance of visible faces in 2D projected images [11], [23]. Locating optimal viewpoints for volumes has been explored by Bordoloi and Shen [12]. They evaluated the balance between the contributions of voxels to pixels in the resultant image using the entropy function. Takahashi et al. decomposed an entire volume into a set of feature components, then compromised between the locally optimal viewpoints for the components to find the globally best viewpoint [13]. Lee et al. and Tao et al. have studied viewpoint selection for flow visualization [14] [15]. Lee et al. proposed a maximum entropy projection buffer to select the streamlines that would cause the minimum occlusion,

³<http://www.honda.co.jp/safetymap/>, (in Japanese)

⁴<http://gmap.dgis.jp/dc/ngt.html>, (in Japanese)

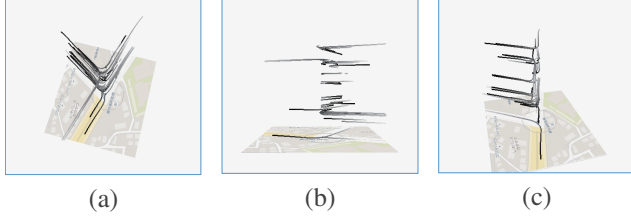


Figure 1. Examples of bad viewpoints. (a) well displaying the structure of trajectories, but crushing the temporal information, (b) well displaying temporal information of trajectories, but not showing the structure of trajectories, (c) not well displaying either shapes or temporal distributions of the trajectories.

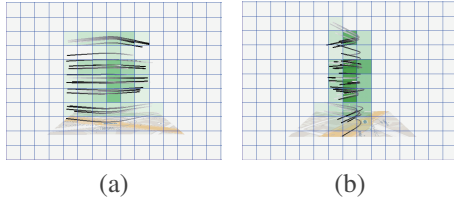


Figure 2. Dividing screen space into tiles to calculate weighted viewpoint entropy. (a) and (b) are visualized results from different viewpoints. Colors of tiles represent the value of $\frac{|s_x|}{S}$ on each tile.

and also proposed a viewpoint selection algorithm that works hand-in-hand with a streamline selection algorithm to maximize the visibility of high complexity regions in the flow field [14]. Although their study complementarily selected streamlines and viewpoints to identify salient flow regions, our study focuses on finding a viewpoint for already displayed trajectories to understand both shapes of trajectories on a map and their distribution on a time axis.

III. VIEWPOINT ENTROPY-BASED APPROACH

“The best viewpoint is the one that obtains the maximum information of a scene. A good view must help us to understand as much as possible the object or scene represented” [11]. What is a good viewpoint in our required system using a space time cube? First, it is one that clearly displays the shapes of trajectories to enable us to understand what kinds of driving situations occur at caution crossroads. Second, it is one that easily enables us to understand the positions of trajectories on a map to observe the surrounding situations. Third, it is one that needs to show the distribution of trajectories on a time axis to understand the time periods in which traffic volume is high. Fourth, it is one for which there is less overlapping of trajectories on the projected screen.

To satisfy the first, third, and fourth requirements, it is desirable that trajectories are widely distributed on the 2D screen. However, if the trajectories are widely spread on the screen, it is sometimes difficult to read their shapes. For examples, Figure 1 (a) well displays the structure of trajectories, but it crushes the temporal information. Figure 1 (b) well displays the temporal information of trajectories, but

it does not show their structures. From our observations, it is hard to understand the shapes and temporal distributions of the trajectories whose projected angles on a 2D screen with a horizontal line are close to vertical as shown in Figure 1 (c). It is easy to understand them if there are many trajectories with loose angles with the horizontal line. Such loose angles also help satisfy the second requirement.

To solve these problems, we adapted an viewpoint entropy-based approach. We divided a screen space into tiles as shown in Figure 2 and computed weighted viewpoint entropy by using the following formula:

$$E = \sum_{x=1..n} \frac{|s_x|}{S} \log_2 \frac{|s_x|}{S} \cdot \log_2 c \lambda_x \quad (1)$$

Each trajectory consists of m segments⁵ to show the trajectory around a crossroad. We counted the number of segments $|s_x|$ passing over each tile x . Here, S means the total number of $|s_x|$. We modified the formula for Shannon’s entropy $E_{noweight} = -\sum_{x=1..n} \frac{|s_x|}{S} \log_2 \frac{|s_x|}{S}$ by weight $\log_2 c \lambda_x$, where c is a constant value. $c \lambda_x$ is defined by the angles of projected segments with the horizontal line in each tile as $\lambda_x = \frac{\sum_{s \in S_x} f(\theta_s)}{L}$, where L is defined by $\sum_{x=1..n} \sum_{s \in S_x} f(\theta_s)$. We assumed that the amount of information was large when the angle was close to 30 degrees, so we defined $f(\theta_s)$ as

$$f(\theta_s) = \begin{cases} -a * \theta_s + b & (\theta_s \leq \theta) \\ a * \theta_s - b & (\text{otherwise}) \end{cases}$$

where $0 \leq \theta_s \leq 90$ ⁶.

Trajectories spreading over the 2D screen simply cause high entropy (viewpoint entropy without weight $E_{noweight}$ in this case). This mainly helps to solve the third requirement, and also helps to solve the first and fourth requirements because it makes it possible to avoid dense projection of trajectories on the 2D screen that crushes the shapes of trajectories and causes occlusions as shown in Figure 2 (b). However, the highest $E_{noweight}$ sometimes causes the situations shown in Figure 1 (b) and Figure 4 (a), which do not preserve the shapes of trajectories. The viewpoint from the top of the hemisphere preserves the shapes of trajectories best. It satisfies the first and second requirements at the same time, but might not satisfy the others as shown in Figure 1 (a). From the comparison shown in Figure 4, we consider that the angles of segments can preserve the shapes of trajectories. We therefore introduced the weight defined by the angle of segments in a 2D screen to solve this tradeoff. θ can control the tradeoff. If we define θ as near 90 degrees, the result might strongly satisfy the first and second requirements, but might not satisfy the others as shown in Figure 1 (a) and sometimes might not satisfy the first and fourth requirements as shown in Figure 1 (c). Although we

⁵ $m = 20$ in this experiment.

⁶ $c = 1, a = 1.0/60, b = 0.5$ and $\theta = 30$ in this experiment.

selected 30 degrees as θ from our observations (such as Figure 4) in this experiment, more detailed investigation through users' evaluations is necessary as a subject for future work.

To search for the optimal viewpoint, we sampled 144 viewpoints from an upper hemisphere surrounding the target STC. We then ranked the viewpoints by the corresponding entropies to select the optimal viewpoint. The viewpoint samples were generated by rotating a viewpoint by 15 degrees up, down, left and right around the center of the STC.

The suitable size of a tile depends on the screen size and the distance between the target STC and the viewpoint. We manually selected the size in this experiment, but we plan to provide a method for automatically finding the suitable tile size in future work.

A. Results of Viewpoint Ranking

We have developed a system for ranking caution crossroads on the basis of vehicle recorder big data, road shapes, and weather information (details are explained in Section V).

We sampled some caution crossroads and verified the viewpoint ranking results calculated by the proposed method. Figure 3 shows the viewpoint ranking results obtained for six types of crossroads, which have characteristic trajectory shapes such as *t*-shaped, *l*-shaped, *s*-shaped, *+*-shaped, *-*-shaped, and *u*-shaped. Each row shows the top three rankings and the worst two rankings of viewpoints for each crossroad, and shows their rankings and values of weighted entropy at the bottom of the images. Each crossroad displays top 30 anomalous operations with 20-second trajectories before and after the operations occurred. The types of trajectory shapes are characterized by anomalous operations other than road shapes.

From the results, we confirmed that the top three viewpoints obviously well display 1) characteristics of trajectories' shapes, 2) positions of trajectories on the map, 3) distribution of trajectories on a time axis, and 4) trajectories with fewer occlusions compared to the worst two viewpoints.

1) *Comparison with No Weight*: Figure 4 shows comparison results for the top ranked viewpoint of the same crossroad by using viewpoint entropy without considering weight $E_{noweight} = -\sum_{x=1..n} \frac{|s_x|}{S} \log_2 \frac{|s_x|}{S}$ and with weight $E = \sum_{x=1..n} \frac{|s_x|}{S} \log_2 \frac{|s_x|}{S} \cdot \log_2 c\lambda_x$. This result clearly shows weight $\log_2 c\lambda_x$ works well for displaying the structure of trajectories from a better viewpoint.

B. Finding Common Optimal Viewpoint for Multiple Crossroads

We extended the proposed method to find an optimal viewpoint for multiple crossroads to compare them from the same angle. It is also used for finding an optimal viewpoint for multiple operations on the same crossroads from the same angle. Because trajectories related to the

braking operations and handling operations are sometimes completely different, finding a common optimal viewpoint is required for observing them from the same direction.

We considered the total of normalized entropies for multiple crossroads. If we consider two crossroads *a* and *b*, common viewpoint entropy E_{common} is described as $E_{common} = E_a/E_{max_a} + E_b/E_{max_b}$. E_{max_a} and E_{max_b} is maximum viewpoint entropy among 144 viewpoints for each crossroad *a* and *b* respectively. E_a and E_b are defined by equation 1.

Figure 5 shows the top three common optimal viewpoints for different crossroad (a) and (b). Each row shows the trajectories on different crossroads from the same viewpoint. These results show the top three viewpoints are completely different, but they are optimal viewpoints for two crossroads.

IV. USERS' EVALUATIONS

To verify the effectiveness of the presented method through users' evaluations, we first manually ranked the viewpoints through Scheffe's paired comparison method, and then measured Spearman's rank correlation coefficient between rankings defined by the proposed method and by users.

We asked nine colleagues (all males, ranging in age between 20 and 50 years) who worked in the computer science domain to evaluate pairs of visualized images taken from ten multiple viewpoints, and obtained their feedback. All of them were familiar with visualization systems, but some of them were not familiar with 3D software. We uniformly sampled ten visualized images from the top ranking viewpoints, selecting two crossroads (Figure 3 (b) and (c)) for evaluation.

It is difficult for users to arbitrarily rank many viewpoints, so we ranked viewpoints by paired comparisons. For this purpose, users scored pairs of viewpoints through the interface shown in Figure 6, where two images and five options appear. These options are linked to the Likert scale; e.g., "the left image is definitely a better viewpoint than the right image" is for option -2, and the complete opposite is option 2. Option 0 is "these two viewpoints are equally good or equally not good."

After that, we ranked ten viewpoints according to Scheffe's method of paired comparisons (Nakaya's modification) [24]. The resulting p-value of the main effect is almost zero. We therefore consider that there is a significant difference among the ten viewpoints.

We next compared viewpoint rankings defined by the proposed method and users' evaluations by using Spearman's rank correlation. In both cases (Figure 3 (b) and (c)), the p-values were below 0.01 (0.00198 and 0.0082) and the rank correlation coefficients were over 0.8 (0.87879 and 0.80606). We therefore consider that there is a positive correlation between the two rankings.

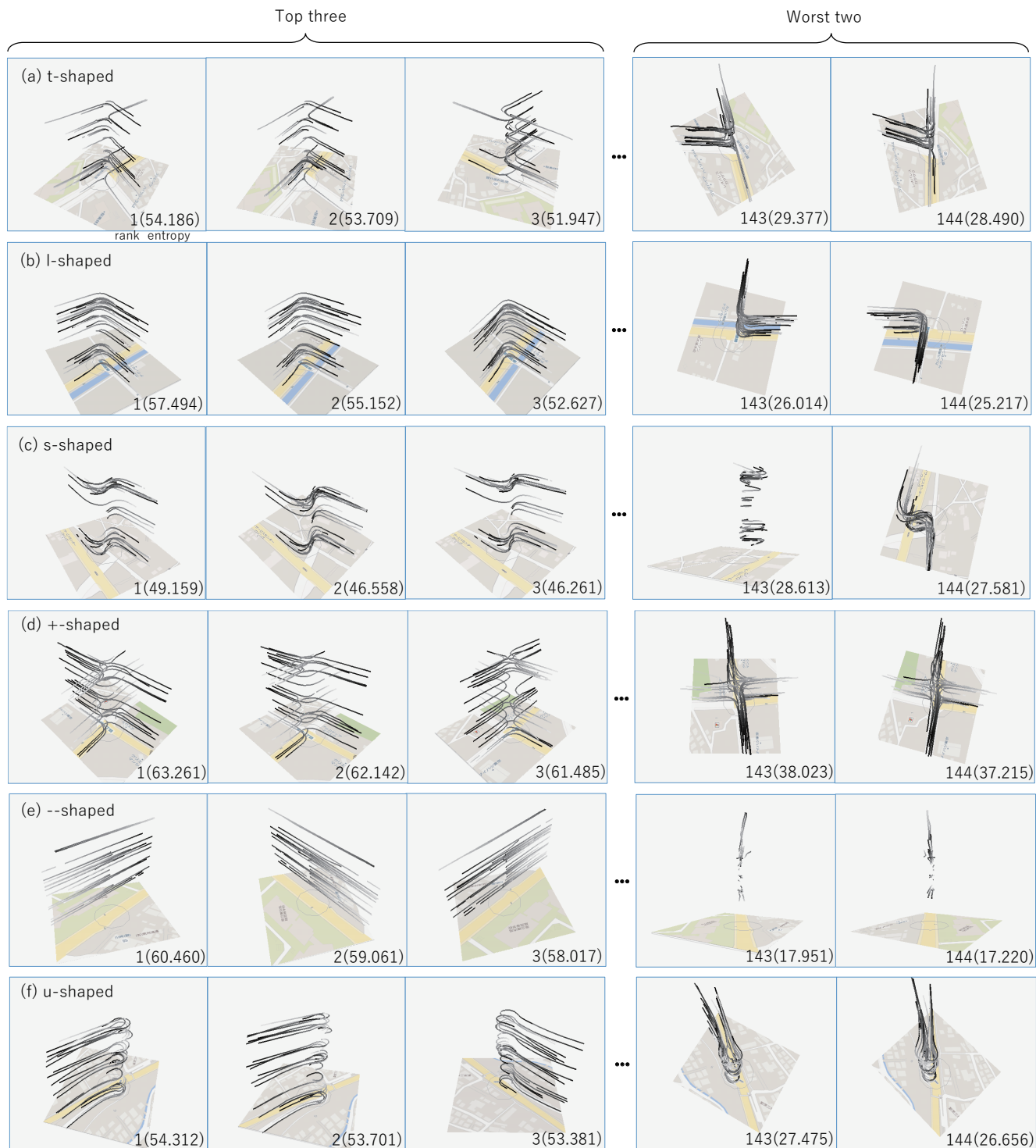


Figure 3. Ranking of viewpoints by proposed viewpoint entropy based methods. Each row represents the results for different types of crossroads having characteristic trajectory shapes: (a) *t*-shaped, (b) *l*-shaped, (c) *s*-shaped, (d) *+*-shaped, (e) *--*-shaped, and (d) *u*-shaped.

Some users commented “It is a very difficult task for me to judge which one is a better viewpoint.”, and “I’m not confident of the results.” Such feedback shows that it is a

fundamentally difficult task for human beings to manually find the optimal viewpoints.

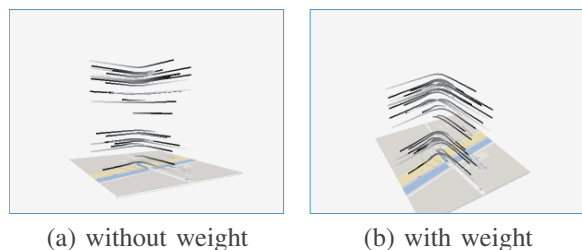


Figure 4. Comparison result of top ranked viewpoint by using entropy without considering weight (a) and with weight (b).

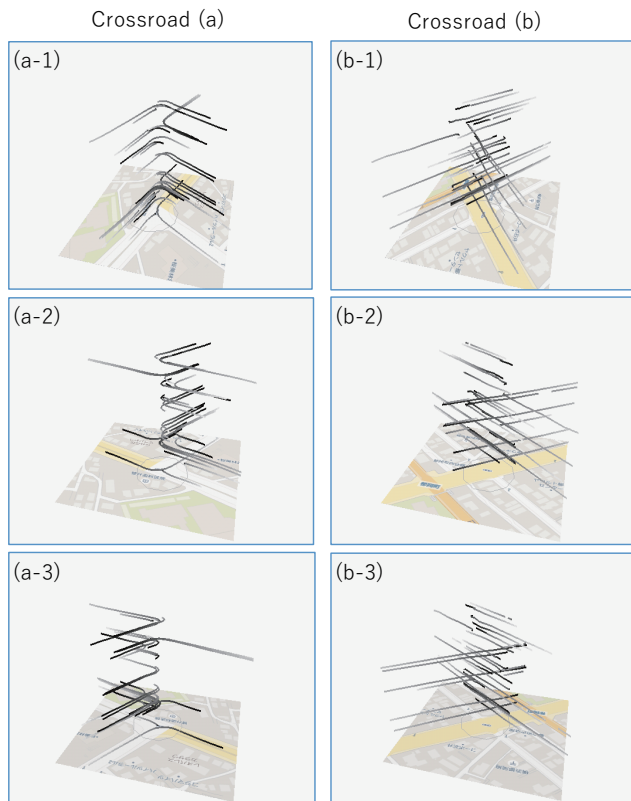


Figure 5. Top three common optimal viewpoints for different crossroads (a) and (b).

V. CASE STUDY

We conducted a case study with large-scale driving records provided by a public transport bus company. The bus company shares catalogs of caution roads with drivers. Since they are based on interviews and reports from drivers, it is tedious and time-consuming to maintain them. We automatically extracted caution crossroads by analyzing the driving records, and provided a catalog of these crossroads created by our proposed visualization method. In this section, we will first describe the driving record dataset and then our method for extracting caution crossroads. Finally, we will show the created catalog and the results we obtained in discussions with bus company personnel.

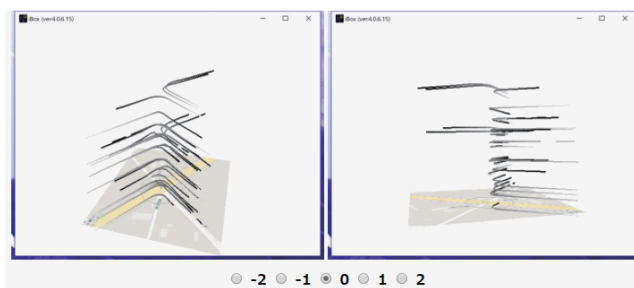


Figure 6. Interface for scoring viewpoints for a pairwise comparison approach. Users compared two viewpoints and scored them in five ranks.

Table I
OPERATION RECORD VARIABLES

Operation	Variables
Braking	date time, latitude/longitude, velocity (V), longitudinal acceleration (Gx), and jerk (derivative of acceleration with respect to time, Jx)
Handling	date time, latitude/longitude, V, yaw velocity (Yr), yaw acceleration, and lateral acceleration (Gy)

A. Dataset

We utilized four datasets for extracting caution crossroads. In addition to the driving record dataset, we used road map, rainfall, and traffic accident datasets. The details are described in the following.

1) *Driving Record Dataset*: In cooperation with a vehicle recorder vendor, Datatec Co., Ltd., we were provided a large-scale driving record dataset from a public transport bus company. The records were collected from over 2,700 drivers for about one month. The bus company uses multifunctional vehicle recorders developed by Datatec that have a longitudinal accelerometer, lateral accelerometer, gyro compass, and GPS. The vehicle recorders captured driving trajectory and status every 0.5 seconds. They also automatically detected basic driving operations such as braking and handling. Several values, including speed and acceleration, were recorded during the operation. The details of the recorded data for each operation are shown in Table I.

2) *Road Map Dataset*: We consider that the characteristics of roads affect driving operations. To extract road information in which each driving operation occurs, we utilized a road map dataset including information about crossroads and roads connecting them. We matched each driving operation with the nearest road segment, and used the road width as one of the road characteristics.

3) *Rainfall Dataset*: We consider that the weather affects road conditions and driving operations. We used X-band Multi Parameter Radar information collected by the Ministry of Land, Infrastructure, Transport and Tourism. It detected rainfall in a 250 m mesh every minute. Since every operation record contained GPS data and time information, we were able to match each operation location with the rainfall information at that time.

4) *Traffic Accident Dataset*: We used traffic accident datasets provided by the bus company and the Institute for Traffic Accident Research and Data Analysis (ITARDA). The bus company dataset included accidents involving its buses in recent years and the ITARDA dataset included accidents resulting in injury or death of involved persons from 2012 to 2014. We used crossroads where these accidents occurred as training samples for classifying caution crossroads.

B. Extracting Caution Crossroads

We have developed a method for detecting crossroads with potential risks. Our method analyzes driving operations occurring at crossroads while taking into account situations such as road width and rainfall. It tries to classify crossroads with/without a history of accidents on the basis of driving record features (e.g., velocity, acceleration, jerk), situations (e.g., road width, rainfall), the number of anomalous operations, and other factors. We utilized several standard classifiers such as logistic regression and SVM. We have omitted the details of features and evaluations here since they are out of scope of this paper.

A crossroad actually has the risk if accidents have occurred at it in recent years. When classifiers detect a crossroad at which no accidents have occurred as one at which accidents have occurred, we can consider it is potentially risky. Usually, classifiers provide their decisions with certain confidence scores, which we use to rank potentially risky crossroads.

C. Catalog Page for Ranked Crossroads

We visualized the 20 top-ranked potentially risky crossroads detected by the method described in Subsection V-B using the dataset described in Subsection V-A. A potentially risky crossroad is one at which no accidents have occurred but has been detected as a caution crossroad by the classifier. We removed some crossroads that were very near railroad stations because driving operations around the stations are always unstable. Each visualization displayed trajectories for the 30 top-ranking anomalous braking or handling operations. Trajectories consisted of 20-second position and time information before and after operations occurred, and were gradually colored from gray to black. The height represents time, with later times at the bottom. To observe the space time cube related to braking and handling operations from the same direction, we selected optimal viewpoints by using the method mentioned in Subsection III-B.

We provided the resulting crossroads ranked as potentially risky to the transport bus company and got feedback from them. We compared our results with their lists of caution spots, which were developed on the basis of drivers' experiences. In so doing, we found that nine crossroads we had classified as potentially risky were included in their lists. Moreover, we were able to point out caution crossroads

that the bus drivers did not recognize. Figure 7 shows the potentially risky crossroads that were included in the bus company's lists of caution spots.

As the result of discussions with stakeholders, we found that the comparison results included the following types of spots ranked as caution spots:

- Spots ranked as caution spots because of cars making sudden lane changes and/or cutting off other cars (Figure 7 (1), (6), and (9))
- Spots ranked as caution spots because of drivers ignoring stop lights or pedestrians and/or bicycles making reckless road crossings (Figure 7 (5), (6), (14), (15) and (19))
- Spots ranked as caution spots because of pedestrians and/or bicycles suddenly appearing from blind spots (Figure 7 (9), (11), and (20))

The bus company personnel also commented that "We observed that a lot of anomalous operations tend to be made in the morning and evening at places where abnormal congestion is likely to occur, such as places near bridges. Such congestion sometimes makes drivers stamp down hard on the accelerator because of impatience, and this causes sudden handling operations as shown in Figure 7 (6), (9), and (15). 3D visualization using a space time cube helps us to observe the differences in abnormalities among hours."

VI. CONCLUSION

We have developed and propose a novel method to select optimal viewpoints for exploring trajectories in a space time cube. We provided an algorithm based on viewpoint entropy weighted by angles of trajectories with a horizontal line on a projected 2D image. As far as we know, there has been no research on viewpoint selection for visualizations of trajectories using an STC. We evaluated the proposed method through users' evaluations and case studies. In the case studies, we generated visualizations of a lot of caution crossroads and discussed them with stakeholders.

We plan to provide a method for automatically finding the most suitable tile sizes. We also plan to evaluate our method by comparing it with other methods such as the one reported by Lee et al. [14]. Utilizing crowdsourcing to gather pairwise comparisons between viewpoints is another possibility for evaluating the results.

ACKNOWLEDGMENT

This work was supported by the Research and Development on Real World Big Data Integration and Analysis program of the Ministry of Education, Culture, Sports, Science, and Technology, Japan.

REFERENCES

- [1] Z. Wang, M. Lu, X. Yuan, J. Zhang, and H. van de Wetering, "Visual Traffic Jam Analysis Based on Trajectory Data," *IEEE Trans. Vis. Comput. Graph.*, vol. 19, no. 12, pp. 2159–2168, 2013.

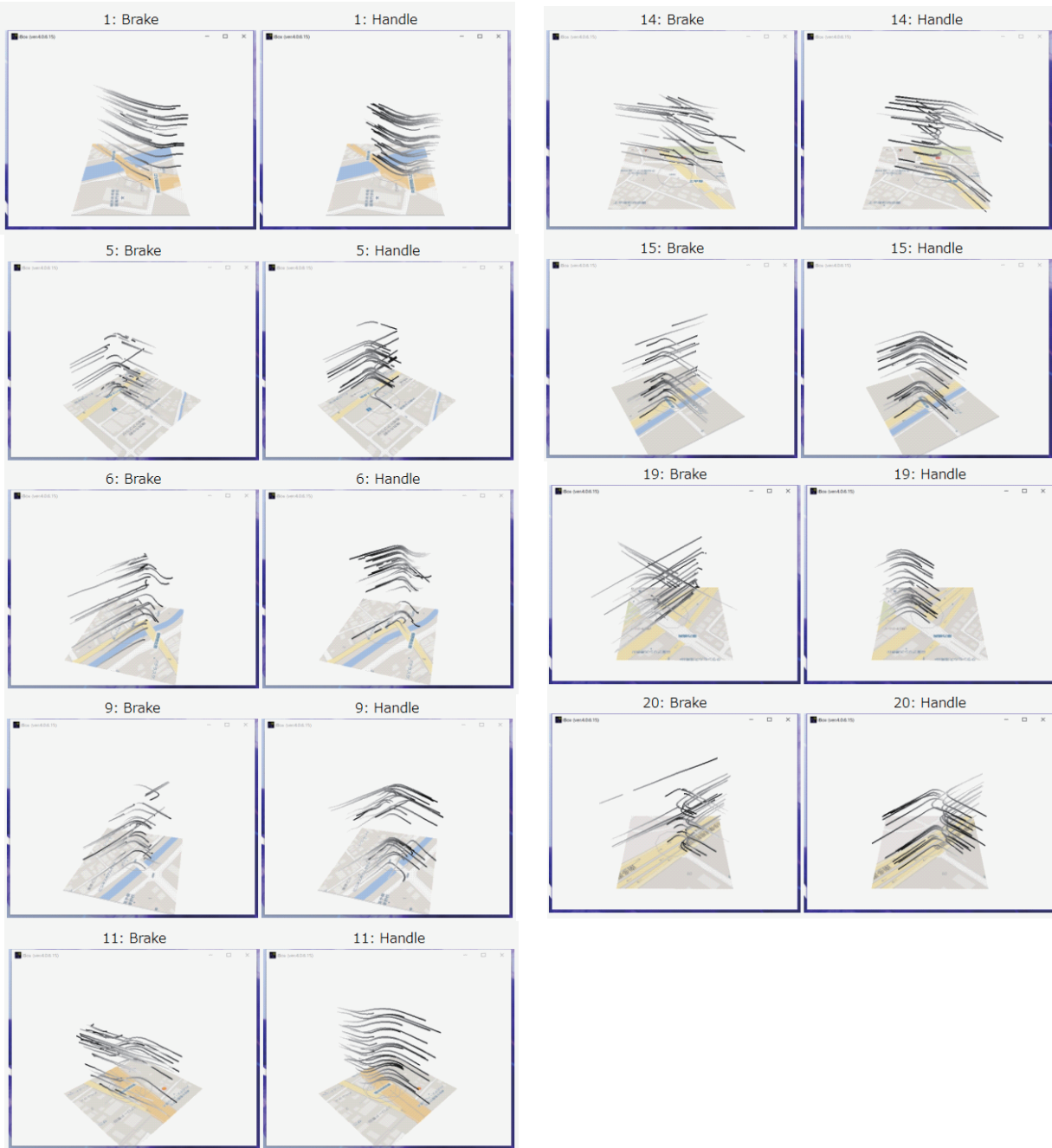


Figure 7. Visualizing trajectories on nine potentially risky crossroads selected from the 20 top-ranked potentially risky crossroads by using the method mentioned in Subsection V-B.

[2] N. Ferreira, J. Poco, H. T. Vo, J. Freire, and C. T. Silva, "Visual Exploration of Big Spatio-Temporal Urban Data: A Study of New York City Taxi Trips," *IEEE Trans. Vis. Comput. Graph.*, vol. 19, no. 12, pp. 2149–2158, 2013.

[3] H. Doraiswamy, N. Ferreira, T. Damoulas, J. Freire, and C. T. Silva, "Using Topological Analysis to Support Event-Guided Exploration in Urban Data," *IEEE Trans. Vis. Comput. Graph.*, vol. 20, no. 12, pp. 2634–2643, 2014.

[4] G. L. Andrienko, N. V. Andrienko, S. Rinzivillo, M. Nanni, D. Pedreschi, and F. Giannotti, "Interactive Visual Clustering of Large Collections of Trajectories," in *Proc. VAST '09*, 2009, pp. 3–10.

[5] G. Andrienko, N. Andrienko, C. Hurter, S. Rinzivillo, and S. Wrobel, "From Movement Tracks through Events to Places: Extracting and Characterizing Significant Places from Mobility Data," in *Proc. VAST 2011*, 2011, pp. 161–170.

- [6] G. L. Andrienko, N. V. Andrienko, P. Bak, D. A. Keim, and S. Wrobel, *Visual Analytics of Movement*. Springer, 2013.
- [7] T. Kapler and W. Wright, “GeoTime Information Visualization,” in *Proc. INFOVIS '04*, 2004, pp. 25–32.
- [8] T. Cheng, G. Tanaksaranond, C. Brunson, and J. Haworth, “Exploratory Visualisation of Congestion Evolutions on Urban Transport Networks,” *Transportation Research Part C: Emerging Technologies*, vol. 36, no. 0, pp. 296 – 306, 2013.
- [9] T. Hägerstrand, “Reflections on “what about people in regional science?”,” *Papers of the Regional Science Association*, vol. 66, no. 1, pp. 1–6, Dec 1989.
- [10] F. Amini, S. Rufiange, Z. Hossain, Q. Ventura, P. Irani, and M. J. McGuffin, “The Impact of Interactivity on Comprehending 2D and 3D Visualizations of Movement Data,” *IEEE Trans. Vis. Comput. Graph.*, vol. 21, no. 1, pp. 122–135, 2015.
- [11] P. Vázquez, M. Feixas, M. Sbert, and W. Heidrich, “Viewpoint Selection using Viewpoint Entropy,” in *Proceedings of the Vision Modeling and Visualization Conference 2001 (VMV-01)*, Stuttgart, Germany, November 21-23, 2001, 2001, pp. 273–280.
- [12] U. Bordoloi and H. Shen, “View Selection for Volume Rendering,” in *VIS 2005*, 2005, pp. 487–494.
- [13] S. Takahashi, I. Fujishiro, Y. Takeshima, and T. Nishita, “A Feature-Driven Approach to Locating Optimal Viewpoints for Volume Visualization,” in *Proc. VIS 2005*, 2005, pp. 495–502.
- [14] T. Lee, O. Mishchenko, H. Shen, and R. Crawfis, “View Point Evaluation and Streamline Filtering for Flow Visualization,” in *Proc. PacificVis 2011*, 2011, pp. 83–90.
- [15] J. Tao, J. Ma, C. Wang, and C. Shene, “A Unified Approach to Streamline Selection and Viewpoint Selection for 3D Flow Visualization,” *IEEE Trans. Vis. Comput. Graph.*, vol. 19, no. 3, pp. 393–406, 2013.
- [16] M. Itoh, D. Yokoyama, M. Toyoda, and M. Kitsuregawa, “Visual Interface for Exploring Caution Spots from Vehicle Recorder Big Data,” in *Big Data 2015*, 2015, pp. 776–784.
- [17] T. T. Elvins, D. R. Nadeau, R. Schul, and D. Kirsh, “Worldlets: 3D Thumbnails for 3D Browsing,” in *Proc. CHI '98*, 1998, pp. 163–170.
- [18] M. Itoh, M. Ohigashi, and Y. Tanaka, “WorldMirror and WorldBottle: Components for Interaction between Multiple Spaces in a 3D Virtual Environment,” in *IV 2006*, 2006, pp. 53–61.
- [19] M. Itoh, J. Fujima, M. Ohigashi, and Y. Tanaka, “Spreadsheet-based Framework for Interactive 3D Visualization of Web Resources,” in *IV 2007*, 2007, pp. 65–73.
- [20] T. J. Jankun-Kelly and K. Ma, “Visualization Exploration and Encapsulation via a Spreadsheet-Like Interface,” *IEEE Trans. Vis. Comput. Graph.*, vol. 7, no. 3, pp. 275–287, 2001.
- [21] E. H. Chi, J. Riedl, P. Barry, and J. A. Konstan, “Principles for Information Visualization Spreadsheets,” *IEEE Computer Graphics and Applications*, vol. 18, no. 4, pp. 30–38, 1998.
- [22] N. Elmqvist and P. Tsigas, “A Taxonomy of 3D Occlusion Management for Visualization,” *IEEE Trans. Vis. Comput. Graph.*, vol. 14, no. 5, pp. 1095–1109, 2008.
- [23] P. Vázquez, M. Feixas, M. Sbert, and W. Heidrich, “Automatic View Selection Using Viewpoint Entropy and its Applications to Image-based Modelling,” *Comput. Graph. Forum*, vol. 22, no. 4, pp. 689–700, 2003.
- [24] S. Nakaya, “A Modification of Scheffe’s Method for Paired Comparisons,” in *Proc. the 11th Meeting of Sensory Test (in Japanese)*, 1970, pp. 1–12.